Highly conductive PEDOT:PSS treated with formic acid for ITO-free polymer solar cells

ARTICLE *in* ACS APPLIED MATERIALS & INTERFACES · JANUARY 2014

Impact Factor: 6.72 · DOI: 10.1021/am405024d · Source: PubMed

4 AUTHORS, INCLUDING:

Desalegn Alemu Mengistie
Chalmers University of Technology
7 PUBLICATIONS **216** CITATIONS
SEE PROFILE

Mohammed Aziz Ibrahem
University of Duhok
9 PUBLICATIONS **109** CITATIONS
SEE PROFILE

Chih Wei Chu
Academia Sinica
169 PUBLICATIONS **4,487** CITATIONS
SEE PROFILE

ACS APPLIED MATERIALS & INTERFACES

Research Article

www.acsami.org

Highly Conductive PEDOT:PSS Treated with Formic Acid for ITO-Free Polymer Solar Cells

Desalegn A. Mengistie,[†,‡,§] Mohammed A. Ibrahem,[†,‡,∥] Pen-Cheng Wang,[§] and Chih-Wei Chu*[,‡,⊥]

[†]Nanoscience and Technology Program, Taiwan International Graduate Program, Academia Sinica, Taipei 115, Taiwan

[‡]Research Center for Applied Sciences, Academia Sinica, Taipei 115, Taiwan

[§]Department of Engineering and Systems Science, National Tsing Hua University, Hsinchu 30013, Taiwan

[∥]Department of Physics, National Taiwan University, Taipei 106, Taiwan

[⊥]Department of Photonics, National Chiao Tung University, Hsinchu 300, Taiwan

Supporting Information

ABSTRACT: We proposed a facile film treatment with formic acid to enhance the conductivity of poly(3,4-ethylenedioxythiophene):poly(styrene sulfonate) (PEDOT:PSS) by 4 orders of magnitude. The effect of formic acid concentration on conductivity was investigated; conductivity increased fast with increasing concentration up to 10 M and then increased slightly, the highest conductivity being 2050 S cm^{-1} using 26 M concentration. Formic acid treated PEDOT:PSS films also exhibited very high transmittances. The mechanism of conductivity enhancement was explored through SEM, AFM, and XPS. Formic acid with its high dielectric constant screens the charge between PEDOT and PSS bringing about phase separation between them. Increased carrier concentration, removal of PSS from the film, morphology, and conformation change with elongated and better connected PEDOT chains are the main mechanisms of conductivity enhancement. ITO-free polymer solar cells were also fabricated using PEDOT:PSS electrodes treated with different concentrations of formic acid and showed equal performance to that of ITO electrodes. The concentrated acid treatment did not impair the desirable film properties as well as stability and performance of the solar cells.

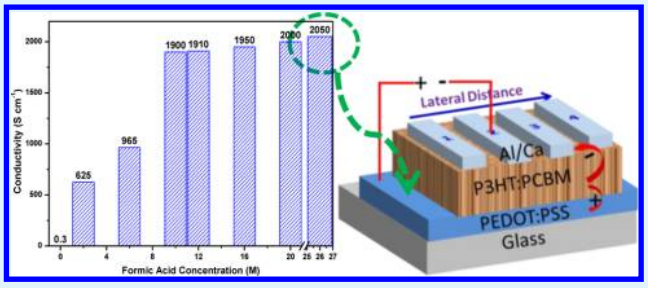

KEYWORDS: *ITO, transparent electrode, PEDOT:PSS, solar cell, formic acid, conductivity enhancement*

1. INTRODUCTION

Flexible organic-based optoelectronic devices such as liquid crystal displays (LCDs), light-emitting diodes (LEDs), solar cells, touch panel displays, and many others have important applications in many areas and have attracted significant interest due to their low-cost, roll-to-roll, and large area processing, mechanical flexibility, and lightweight properties.[1,2] The roll-to-roll processability, which also is a determining factor for the cost of devices, is highly dependent on electrodes of the devices as the interlayer and active layer materials can easily be processed through conventional solution processing. Optoelectronic devices need at least one transparent electrode in order to allow light to be harvested by the active layer or to emit light. Tin doped indium oxide (ITO), which currently is used as the standard transparent electrode, has many drawbacks: ITO's price is skyrocketing due to Indium's limited availability, is mechanically brittle, and has poor adhesion on organic and polymeric materials.[3,4] For example, 37−50% of materials cost in polymer solar cells is from ITO.[5] ITO has also additional inherent problems such as release of oxygen and indium into the organic layer, poor transparency in the blue region, and complete crystallization of ITO films, which requires high temperature processing.[6] To respond to these drawbacks, numerous solution processable and printable candidates including metal nanowires,[7,8] carbon nanotubes,[9−11] graphene,[12,13] and conducting polymers[14−18] are being actively investigated as a replacement for ITO.

Among the alternatives, conductive polymer poly(3,4-ethylene dioxythiophene) (PEDOT) doped with poly(styrene sulfonate) (PSS) (chemical structure shown in Figure 1) is quite promising as a next-generation transparent electrode material. PEDOT:PSS films have high transparency in the visible range, high mechanical flexibility, and excellent thermal stability and can be fabricated through conventional solution processing. Furthermore, PEDOT:PSS films can be easily nanostructured to enhance the localized light intensity to the active layer and generate more power.[19] However, pristine PEDOT:PSS films suffer from very low conductivity of less than 1 S cm^{-1}, which is too low to be used as standalone electrodes. PEDOT is insoluble in most solvents but can be dispersed in water by using PSS as a counterion. PSS also serves as an excellent oxidizing agent, charge compensator, and as a

Received: September 12, 2013
Accepted: January 24, 2014
Published: January 24, 2014

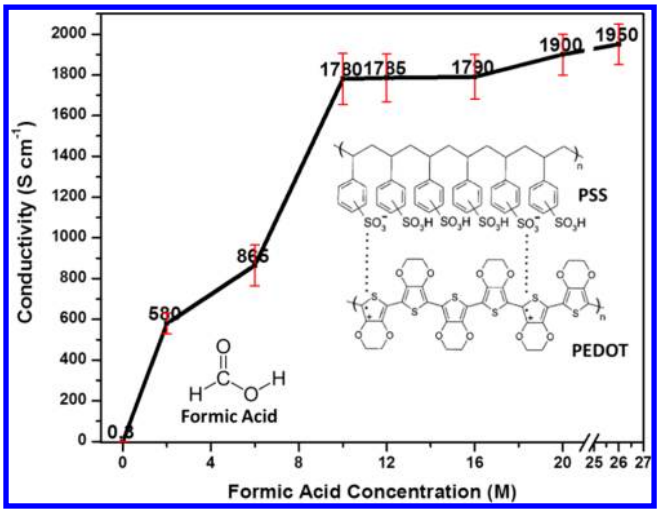

Figure 1. Average conductivities of PEDOT:PSS films treated with different concentrations of formic acid with error bars. Inset: chemical structure of PEDOT:PSS and formic acid.

template for polymerization.[20,21] However, in an aqueous dispersion of PEDOT:PSS, short PEDOT chains are surrounded by a thin PSS-rich surface layer, which is one of the main reasons for its low conductivity.

Many techniques have been proposed and are being actively investigated to enhance the conductivity of PEDOT:PSS by more than 3 orders of magnitude to replace ITO.[22] The approaches include addition of organic compounds such as ethylene glycol, polyethylene glycol, dimethyl sulfoxide, dimethyl sulfate, sorbitol, mannitol, ionic liquid, anionic surfactant, etc. into the PEDOT:PSS aqueous dispersion,[23−30] treatment of PEDOT:PSS films with polar organic compound, alcohol, salt, acid, zwitter ion, or cosolvents,[31−35] or a combination of both mixing the additive in the PEDOT:PSS dispersion and film treatment.[36] Recently, the conductivity of Clevios PH1000 PEDOT:PSS has been enhanced to 3065 S cm^{-1} by treating the film three times with 1 M sulfuric acid at 160 °C and to 3400 S cm^{-1} using vacuum vapor phase polymerization technique.[37,38] However, the polymer solar cell device performances fabricated with these high conductivity PEDOT:PSS anodes were lower than the ITO counterparts. In addition to high conductivity, high transmittance and other film properties should not be impaired during film treatment. Hence, further investigations on the mechanism of conductivity and other film properties are vital. Takano et al. used small and wide-angle X-ray scatterings and found that nanocrystals of PEDOT are formed after film treatment.[39] Wei et al. also showed that there is improved crystallinity of the PEDOT and the ordering of the PEDOT nanocrystals in solid films after film treatment with EG which led to both carrier concentration and carrier-mobility enhancement.[40]

In our earlier report, we showed conductivity enhancement of PEDOT:PSS to 1362 S cm^{-1} by simple film treatment with methanol and investigated in detail the mechanisms of conductivity enhancement.[31] In this work, we report conductivity enhancement of Clevios PH1000 PEDOT:PSS by treating with formic acid and its application as transparent anode for ITO-free polymer solar cells (PSCs). Treatment with different concentrations of formic acid was carried out by dropping formic acid at 140 °C on annealed PEDOT:PSS film with or without subsequent rinsing with water. The highest conductivity was 625, 1900, and 2050 after treatment with 2, 10, and 26 M formic acid, respectively. High dielectric constant formic acid easily screens the Coulombic interaction between PEDOT and PSS and brings about phase separation between them leading to more aggregated and interconnected PEDOT chains which facilitate easy charge transfer. ITO-free PSCs with formic acid treated anodes also showed almost equal power conversion efficiency to that of the ITO counterparts.

2. EXPERIMENTAL SECTION

2.1. Preparation and Characterization of PEDOT:PSS Films. Clevios PH1000 PEDOT:PSS aqueous dispersion (Heraeus Ltd.) has PEDOT:PSS concentration 1.0−1.3% by weight, and the weight ratio of PSS to PEDOT is 2.5. Glass substrates with area 1.5 × 1.5 cm^2 were cleaned with sonicator successively in detergent water and twice in deionized water for 15 min each time and then dried in an oven after purging with N_2 air. PEDOT:PSS filtered through 0.45 μm PTFE syringe filter was spin coated at 3000 rpm for 60 s on glass substrates which were treated with UV/ozone for 15 min prior to spin coating. The films were annealed on a hot plate in ambient atmosphere at 130 °C for 20 min, and film treatment was performed inside a hood by dropping 150 μL of different concentrations of formic acid (Sigma Aldrich) on the film at 140 °C and then dried for 5 min. For some of the films rinsing was done, after cooling the annealed films, by briefly dipping in DI water three times and then were dried at 140 °C for 5 min. For some films formic acid treatment was repeated three times by rinsing after each treatment. Thicker PEDOT:PSS films were prepared by spin coating multiple times, and annealing and film treatment were done after each layer.

Film thickness was measured using alpha step surface profiler (Veeco Dektak 150). Conductivities were measured using van der Pauw four-point probe technique with Hall Effect measurement system (Ecopia, HMS-5000). Absorption and transmission spectra of the films were measured using a Jacobs V-670 UV-vis-NIR spectrophotometer. The values of transmittances reported in this paper are at the wavelength of 550 nm and include the absorption of the glass substrate. For absorption measurement quartz substrates were used to prepare the films. X-ray photoelectron spectroscopy (XPS) was done using PHI 5000 VersaProbe (ULVAC-PHI, Chigasaki, Japan) equipped with Al Kα X-ray source (1486.6 eV). Surface morphologies of the films were imaged using a scanning electron microscope (SEM) (FEI Nova 200) and an atomic force microscope (AFM) (Veeco di Innova) in the taping mode. Work function measurements were performed using a low-energy photoelectron spectrometer (AC-2, Riken-Keiki). AC-2 works at atmospheric pressure in ambient atmosphere having an open counter equipped with a UV source.

2.2. Fabrication and Characterization of PSCs. PSCs were fabricated using both ITO-free highly conductive formic acid treated PEDOT:PSS films and ITO (<7 Ω □$^{-1}$, RiT display) anodes on glass. A relatively well studied and stabilized donor:acceptor blend of poly(3-hexylthiophene) (P3HT) and [6,6]-phenyl-C_{61}-butyric acid methyl ester ($PC_{61}BM$) was used as the active layer. A blend solution of P3HT:PCBM was prepared by dissolving 20 mg mL^{-1} of each component in 1,2-dichlorobenzene at 70 °C for 3 h and spin coated at 600 rpm for 60 s in a N_2 filled glovebox on the PEDOT:PSS film treated with formic acid and ITO. Less conductive PEDOT:PSS (Clevios P VP 4083) was spin coated at 4000 rpm for 60 s on ITO surface as a buffer layer and annealed in the same way prior to the active layer deposition. The active layer was then solvent annealed by covering with glass Petri dishes for 30 min, and, subsequently, the films were annealed on a hot plate at 130 °C for 30 min. The devices were completed by thermal deposition of 30 and 60 nm thick calcium and aluminum, respectively, at a pressure below 10^{-6} Torr through a shadow mask.

The photovoltaic performance of the devices was measured inside a glovebox filled with N_2 under simulated AM 1.5G illumination (100 W cm^{-2}) using a xenon lamp based solar simulator (Thermal Oriel 1000 W). The light intensity was calibrated by a monosilicon photodiode

with a KG-5 color filter (Hamamatsu, Inc.). Devices were illuminated under mask, and the active area of the devices was controlled to be 0.1 cm^2.

3. RESULTS AND DISCUSSION

3.1. Conductivity, Optoelectronics Properties, and Other Characterizations of the PEDOT:PSS Films. The

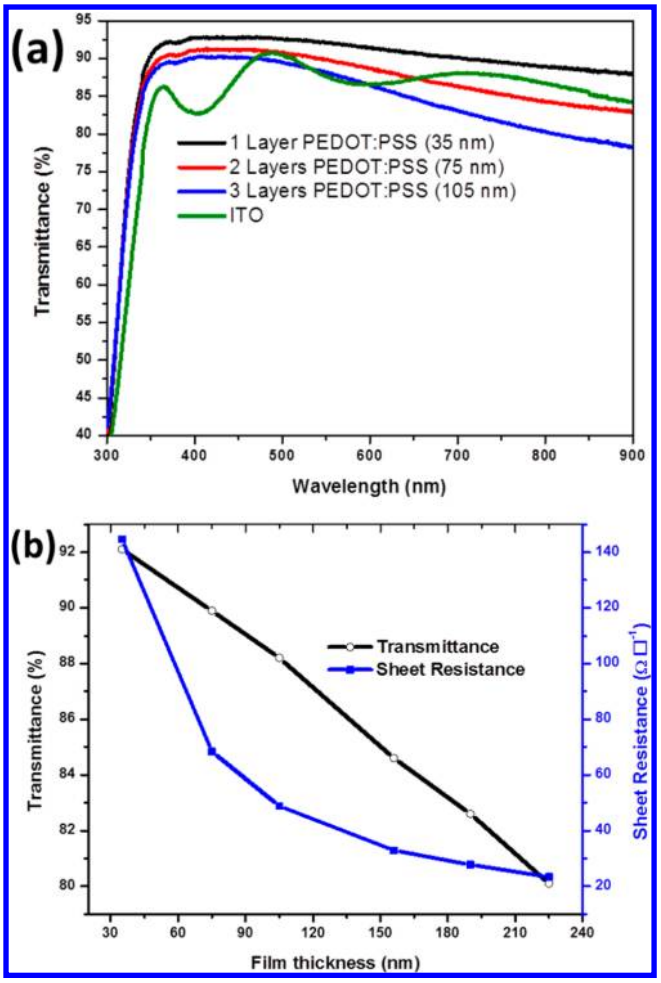

Figure 2. (a) Transmittance of l, 2, and 3 layers of PEDOT:PSS films treated with 26 M formic acid and ITO. (b) Variation of transmittance and sheet resistance with film thickness for PEDOT:PSS treated with 26 M formic acid.

conductivities of PEDOT:PSS films treated with different concentrations of formic acid are shown in Figure 1 along with the error bars. The conductivity increased very fast up to 10 M formic acid concentration and increased only slightly afterward. The average conductivity was 0.3, 580, 1780, and 1950 S cm^{-1} for pristine, 2, 10, and 26 M (98% v/v concentration) formic acid concentration, respectively. The average conductivity was calculated by measuring at least different 10 samples. The highest conductivity observed was 625, 1900, and 2050 S cm^{-1} for 2, 10, and 26 M formic acid concentration, respectively. This conductivity is comparable to the value reported by Xia et al. using 1.5 M sulfuric acid by a single treatment.[37] The same authors also used organic acids (acetic acid and higher molecular weight acids) to treat Clevios P and showed "n" shaped conductivity enhancement with acid concentration where the maximum conductivity was 210 S cm^{-1}.[33] They did not find appreciable conductivity enhancement with pure acids.

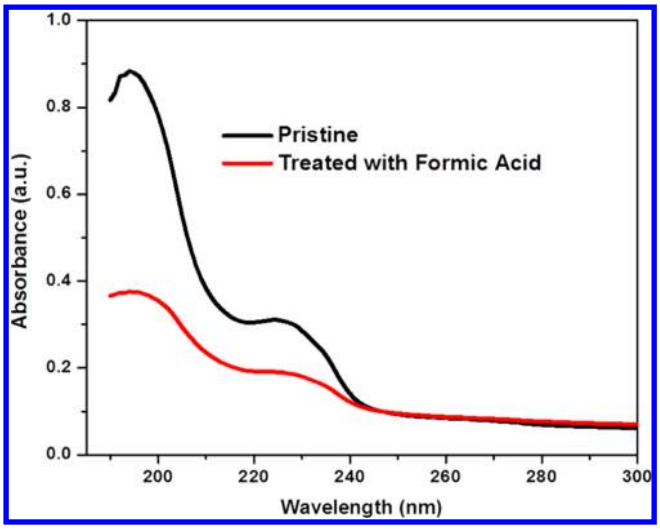

Figure 3. UV absorption spectra of PEDOT:PSS films before and after formic acid treatment.

However, our observation is in contrary to this, and even the highest conductivity was shown using almost pure formic acid. Yoo et al. also improved the conductivity of PEDOT:PSS to 250 S cm^{-1} using preheated dichloroacetic acid.[41]

Conductivity enhancement is strongly dependent on dielectric constants of the chemicals used for treatment; solvents with higher dielectric constants induce a stronger screening effect between counterions and charge carriers, which in turn reduces the Coulomb interaction between positively charged PEDOT and negatively charged PSS dopants.[42] The dielectric constant of sulfuric acid, formic acid, and acetic acid is 101, 58.5 and 6.2, respectively, and is in agreement with the conductivity enhancement imparted by the acids.[43,44] The high dielectric constant formic acid facilitates the segregation of PSS from the film. As shown in the SEM images in Figures S1b and S1c (Supporting Information), darker segregated lines are formed after formic acid treatment which are similar to the methanol treatment.[31] These lines are insulator PSS and were easily removed by rinsing with DI water (Figure S1d, Supporting Information). The film thickness decreased by 20 to 25 nm after treatment. We also noted that there was almost no change in conductivity after rinsing with DI water; rather we sometimes experienced some film damages by the highly hydrophilic water. The PSS was only physically present on the film surface but functionally separated. In an effort to further enhance the conductivity, we tried three times treatment by rinsing after each step as reported by Xia et al.,[37] but there was no appreciable change in conductivity. The film was seen more compact and chains shorter as will be discussed later using AFM images.

Conductivity is related to mobility and bulk concentration with the following formula[45]

$$\sigma = e\mu N \quad (1)$$

where σ, e, μ, and N are conductivity, elementary charge, carrier mobility, and bulk concentration, respectively. As measured by the Hall effect measurement system, the bulk concentration of PEDOT:PSS films increased from 10^{17} cm^{-3} to 10^{21} cm^{-3} after film treatment. This carrier concentration is equal or even a little higher than that of ITO. The bulk concentration for semimetals is in the order of 18 to 21 cm^{-3} and that of metals more than the order of 22 cm^{-3}. However, the mobility was

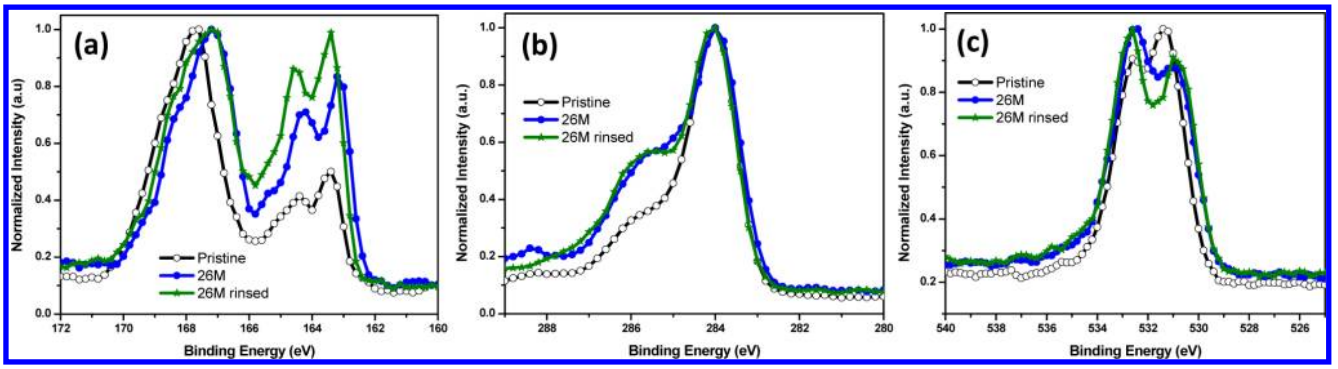

Figure 4. XPS spectra of pristine PEDOT:PSS and PEDOT:PSS films treated with 26 M formic acid (26 M − before rinsing and 26 M rinsed − after rinsing). (a) S(2p), (b) C(1s), and (c) O(1s) core-level spectra.

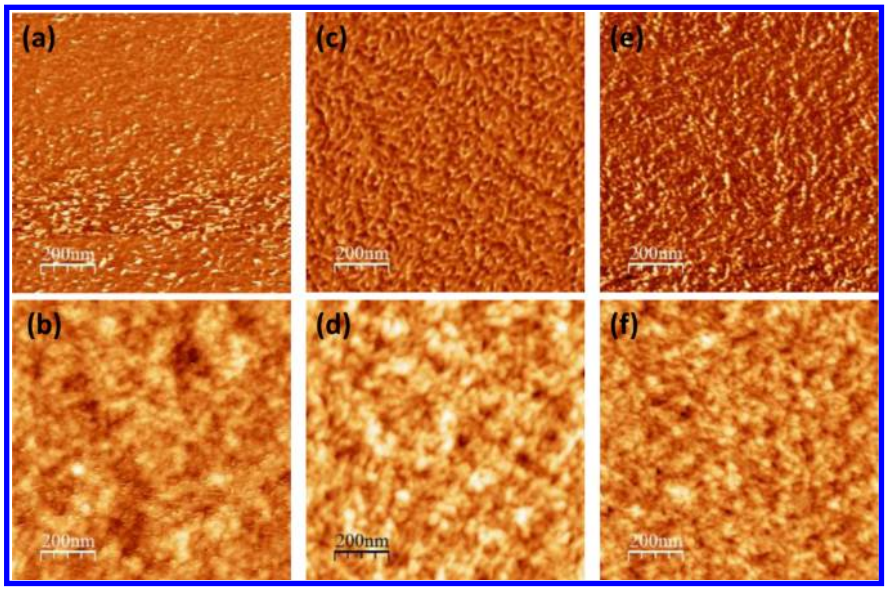

Figure 5. AFM images of PEDOT:PSS films: pristine (a) and (b), treated with 26 M formic acid and rinsed with DI water once (c) and (d) and treated with 26 M formic acid and rinsed with DI water three times (e) and (f). The upper images are phase images, and the bottom ones are topographic images. All the images are 1 μm × 1 μm.

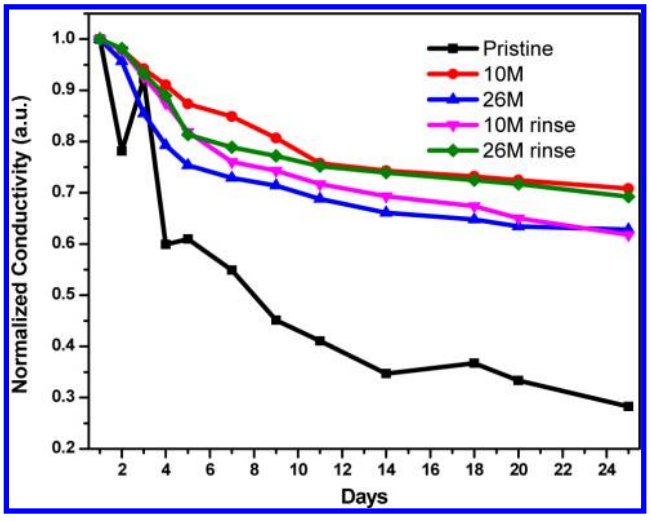

Figure 6. Conductivity stabilities of pristine and 10 and 26 M formic acid (both before and after rinsing) treated PEDOT:PSS films in the ambient atmosphere.

seen not to be enhanced much, fluctuating between 0.1 to 5 $cm^2\ V^{-1}\ s^{-1}$ both before and after treatment. The conductivity value, however, is the same even with these fluctuations. Recently, Wei et al. measured the mobility of PEDOT:PSS films using ion-gel transistors combined with in situ UV−vis−NIR spectroscopy and showed that mobility increased after EG treatment although they also pointed out that the exact value will have errors.[40] Mobility measurement of PEDOT:PSS using the Hall effect is challenging since the high carrier concentration produces small Hall voltage and mobile ions, and the values obtained were seen to fluctuate.

Formic acid treatment did not impair the transmittance of the PEDOT:PSS films. Figure 2a shows the transmittance spectra of one, two, and three layers of PEDOT:PSS films on glass treated with formic acid and ITO on glass. Even three layers of PEDOT:PSS film (~100 nm thick) has higher transmittance than ITO in the violet, blue, and green regions. The transmittance values of one, two, and three layers of PEDOT:PSS and ITO are 92.1, 89.9, 88.2, and 88%, respectively, at 550 nm including the glass substrate. Figure 2b shows the variation of sheet resistance and transmittance with film thickness. The transmittance decreases almost linearly with increasing film thickness. The sheet resistance was 145, 68, and 23 $\Omega\ \square^{-1}$ for film thickness 35, 75, and 225 nm, respectively, while the transmittance was 92.1, 89.9, and 80.1%,

dx.doi.org/10.1021/am405024d | ACS Appl. Mater. Interfaces 2014, 6, 2292−2299

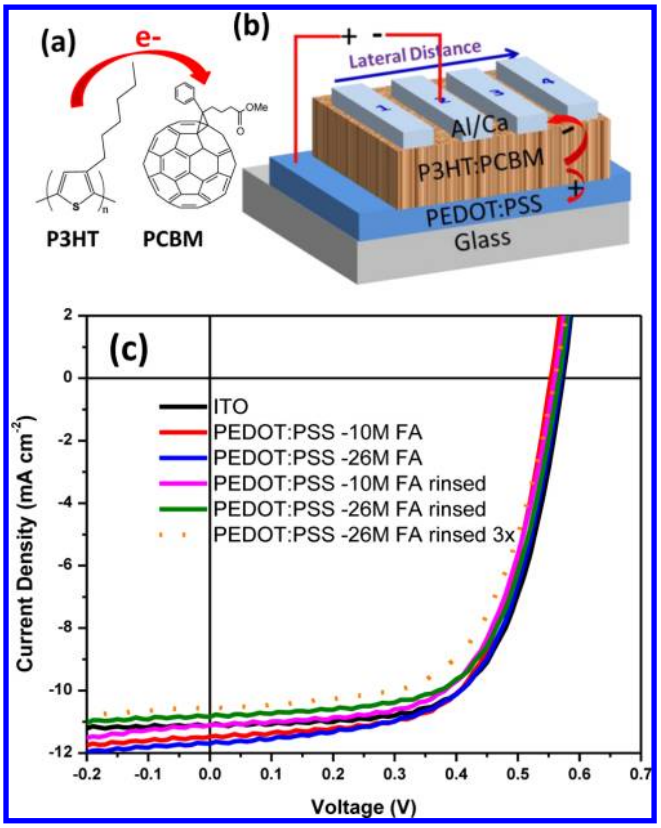

Figure 7. (a) Chemical structures of active layer chemicals. (b) Device architecture of the ITO-free PSC. (c). J-V curves of PSCs with ITO and PEDOT:PSS treated with 10 and 26 M formic acid before and after rinsing. (26 M rinsed 3× – treatment done three time with 26 M formic acid).

respectively. Three layers of PEDOT:PSS film treated with formic acid fulfill the minimum optical and electrical requirements for transparent electrodes which are transmittance higher than 90% and sheet resistance less than 100 Ω $\square^{-1}$ ensuring that PEDOT:PSS films are promising replacements for ITO electrodes. For transparent electrodes, transmittance and sheet resistance are related by the following formula[46]

$$T = \left(1 + \frac{Z_0\sigma_{op}}{2R_S\sigma_{dc}}\right)^{-2} \quad (2)$$

where T is the transmittance, R_S is the sheet resistance, Z_0 = 377 Ω is the impedance of free space, and σ_{op} and σ_{dc} are the optical and dc conductivities, respectively. The minimum industry standard is $\sigma_{dc}\sigma_{op}^{-1} > 35$. The $\sigma_{dc}\sigma_{op}^{-1}$ is calculated for different thicknesses and given in Table S1 (Supporting Information). Formic acid treated PEDOT:PSS films have $\sigma_{dc}\sigma_{op}^{-1} > 104$ and even higher for lower film thicknesses rivaling any other reported values.[36]

To further explore the effect of formic acid and the mechanism of conductivity enhancement, we utilized various characterizations. The UV absorption spectra of PEDOT:PSS film decreased after formic acid treatment (Figure 3). The two absorption bands originate from the aromatic rings of PSS.[16,36] The decrease in the UV absorption spectra and 20–25 nm film thickness reduction after formic acid treatment is attributed to the removal of PSS from the film.

The removal of PSS from the PEDOT:PSS film was further confirmed and quantified using XPS. Figure 4 shows the XPS spectra of pristine PEDOT:PSS and those treated with 26 M formic acid both before and after rinsing with DI water. The S(2p) peak at the binding energy of 167.6 eV corresponds to the sulfur signal of PSS, and the doublet peaks at 164.4 and 163.4 eV correspond to the sulfur signal of PEDOT (Figure 4a).[47] The peaks were shifted a little bit to the lower energy level after formic acid treatment. The PEDOT:PSS ratio was calculated by calculating the area under each peak using full width at half-maximum (FWHM) curve fitting. The ratio of PEDOT to PSS increased from 1:2.83 before film treatment to 1:1.23 after film treatment by dropping formic acid only and even increased further to 1:1.07 after rinsing with DI water; which is 56.5% and 62%, respectively, PSS removal from the film surface. This is the highest PSS removal to the best of our knowledge. This high percentage removal of PSS, however, may not be from the entire volume of the film as formic acid will not penetrate entirely, and even if it did it will be difficult for long chain PSS to come up to the film surface. The PEDOT to PSS ratio of 1:2.83 for the pristine film agrees well with the already accepted idea that the film surface contains more PSS than the bulk.[48] Almost the same amount of PSS loss was also observed using 10 M formic acid treatment as shown in Figure S2 and Table S2 (Supporting Information). The removal of PSS from the film surface did not affect much the work function of the films (Figure S3, Supporting Information). Formic acid with its high dielectric constant induces a screening effect between the positively charged PEDOT chains and negatively charged PSS chains, thus reducing the Coulombic interaction between them.[42] The reduction of the Coulombic interaction between PEDOT and PSS chains facilitates phase separation on the nanometer scale. Moreover, the polar hydrophilic formic acid will also easily dissolve the phase separated hydrophilic PSS and facilitate its removal from the film.

The C(1s) and O(1s) core level spectra of pristine and formic acid treated PEDOT:PSS films are shown in Figures 4b and 4c. A new small and broad shoulder peak appeared around 285.6 eV after formic acid treatment in the C(1s) spectra. This new peak at higher energy could be the C═O peak which has come from formic acid. The two peaks in Figure 4c at 532.6

Table 1. Photovoltaic Performances of PSCs with ITO and PEDOT:PSS Treated with 10 M and 26 M Formic Acid (before and after Rinsing) Anodes Extracted from the J-V Curves

anode	J_{SC} (mA cm^{-2})	V_{OC} (V)	FF (%)	PCE (%)	R_S (Ω cm^2)	R_{SH} (KΩ cm^2)
ITO	11.12	0.57	64.84	4.11	1.1	2.96
PEDOT:PSS – 10 M FA	11.48	0.56	63.31	4.07	2.85	2.56
PEDOT:PSS – 26 M FA	11.70	0.57	61.48	4.10	2.71	2.68
PEDOT:PSS – 10 M FA rinsed	11.10	0.56	62.90	3.91	2.96	1.82
PEDOT:PSS – 26 M FA rinsed	10.84	0.57	63.6	3.93	2.82	2.51
PEDOT:PSS – 26 M FA rinsed 3×	10.55	0.56	61.1	3.61	4.12	1.93

and 531.4 eV are the O peaks from PEDOT and PSS, respectively. The PSS peak became smaller and broadened to the lower energy level after formic acid treatment which could be due to H^+ reacting with PSS^- forming PSSH. These suggest that there is deprotonation of formic acid at high treatment temperature even at higher formic acid concentration. The anion and cation of formic acid will interact with the positively charged PEDOT and negatively charged PSS, respectively and facilitate the phase separation between PEDOT and PSS.

The AFM images show that there is clear change in the film morphology after treatment with formic acid (Figure 5). In the phase image, the brighter (positive) and dark (negative) phase shifts correspond to PEDOT-rich grains and PSS-rich grains, respectively.[49] The phase image is homogeneous with disconnected PEDOT-rich chains and weak phase separation between PEDOT and PSS for the pristine films, whereas there is a good phase separation between PEDOT and PSS chains with more fiber-like interconnected conductive PEDOT-rich chains after film treatment with formic acid. The pristine film is covered with more PSS-rich and the formic acid treated film with PEDOT-rich domains. The depletion of insulating PSS leads to a 3D conducting network of highly conductive PEDOT, resulting in an increase in the conductivity. The topographic AFM images show that the films were quite smooth with rms roughness of 1.31, 1.66, and 1.89 nm before and after treatment with formic acid once and three times, respectively. Even though PEDOT chains were seen to be more aggregated after formic acid treatment, they were not as big as it happened to EG treatment.[30] When formic acid treatment was done three times the grain sizes became even smaller, probably that is one of the reasons why conductivity did not increase with three times treatment. The films were also seen to be more compacted after treatment. The compact and fiber-like PEDOT-rich grains facilitate charge conductivity.

Earlier reports showed that there is improved crystallinity and ordering of the PEDOT nanocrystals[40] and conformation change of PEDOT chains from a coiled to a linear/extended-coil structure[50] after EG treatment of PEDOT:PSS. The phase separated, fiber-like, and interconnected PEDOT-rich chains in the AFM phase images suggest that the conformation of PEDOT will be changed. In the untreated solid film, PEDOT and PSS are held by Coulombic attractions and have coiled or core−shell structure with a hydrophobic conductive PEDOT-rich core and a hydrophilic insulating PSS-rich shell which is formed due to repulsion between long PSS chains in the outer shell.[49] Formic acid treatment with high dielectric constant screens the Coulombic attraction between PEDOT and PSS chains leading to phase separation between them, and PEDOT chains will be linearly oriented and interconnected to each other. The phase separated, crystalline, and oriented PEDOT polymer chains allow more interchain interaction between the conducting polymers. Hence, the energy barrier for interchain and interdomain charge hopping will be lowered leading to better charge transfer among the PEDOT chains. Charge hopping among the polymer chains is believed to be the dominant conduction mechanism in conducting polymers.[51] PEDOT-rich chains with improved crystallinity, preferred orientation, linear structure, larger grain size, and lower intergrain hopping promote the charge hopping, and eventually the conductivity is tremendously enhanced.

A question may be raised whether acid treatment will affect the stability of the film or not. In principle, the removal of the insulator hygroscopic PSS from film surface should not only increase the conductivity of the film but also improve its long-term stability as PSS is the prime reason for the degradation of organic solar cells.[31,36] Moreover, formic acid with a low boiling point (~101 °C) will evaporate after treatment. As a proof of concept, we assessed the conductivity stability of the PEDOT:PSS films by keeping them in ambient atmosphere at room temperature and humidity higher than 75%. As expected, formic acid treated films maintained 70% of the original conductivity, while the pristine films maintained only 28% in 25 days (Figure 6). The detail mechanism of degradation needs some further investigation.

3.2. ITO-Free PSCs Using PEDOT:PSS Treated with Formic Acid. To evaluate device performances, PSCs using PEDOT:PSS treated with 10 and 26 M formic acid both before and after rinsing as standalone anodes were fabricated. The chemical structures of the active layer chemicals (P3HT and $PC_{61}BM$), device architecture, and the current density (J)-voltage (V) curves of the PSCs with single layer (~35−45 nm) PEDOT:PSS anodes are shown in Figure 7. PSCs using the ITO anode with a less conductive PEDOT:PSS (Clevios P VP Al 4083) buffer layer were also fabricated as control devices. The power conversion efficiency (PCE), short-circuit current density (J_{SC}), open-circuit voltage (V_{OC}), fill factor (FF), and series resistance (R_S) and shunt resistance (R_{SH}) of the PSCs are given in Table 1. Generally, PEDOT:PSS anodes show almost equal performance to that of the ITO anode owing to their high conductivity and high transmittances. The PEDOT:PSS anode treated with 26 M formic acid showed a J_{SC} of 11.70 mA cm^{-1}, V_{OC} of 0.57 V, and PCE of 4.10% with a FF of 61.48%. The PSC with reference ITO electrode has a PCE of 4.11% with little higher FF and lower J_{SC}. Both 10 and 26 M treated PEDOT:PSS anodes showed better J_{SC} than their ITO counterparts due to their higher transmittance values. When rinsing was done for both 10 and 26 M formic acid, the device performance was a little lower. For the film treated with only a drop method (without further rinsing with DI water), a very thin PSS layer segregated by formic acid is still on the film surface, and it will act as a functional buffer layer giving an electron blocking function for the device. Additionally, the rough surface after drop treatment may serve as a center for the initial crystallization of the P3HT polymer which further leads to better alignment of P3HT and PCBM domains.[52] When treatment was done three times, the performance was lower probably due to the unfavorable film condition during repeated water rinsing. PEDOT:PSS electrodes showed low R_S and high R_{SH} values comparable to the ITO electrode. The preliminary stability of the devices was assessed by keeping them in the N_2 filled glovebox. Devices with formic acid treated PEDOT:PSS anodes maintained up to 93% of the original efficiency in fourteen days, while those with the ITO anode maintained only 86% (Figure S4, Supporting Information). The same trend was also observed in our earlier studies for PEDOT:PSS treated with methanol anodes.[31] The highly acidic PSS buffer layer corrodes ITO and is the main reason for fast degradation of the ITO deices.[53]

4. CONCLUSIONS

We have shown, for the first time, almost 100% concentrated acid can tremendously enhance conductivity of PEDOT:PSS by simple film treatment without affecting its other desirable properties. The conductivity was enhanced from 0.3 S cm^{-1} to 1900 and 2050 S cm^{-1} after film treatment with 10 and 26 M formic acid, respectively. Formic acid treated PEDOT:PSS films

also have very high transmittances: 92.1% with 145 Ω $\square^{-1}$ sheet resistance and 80.1% with 23 Ω $\square^{-1}$ sheet resistance. Four orders of magnitude carrier concentration enhancement, phase separation between PEDOT and PSS, removal of PSS from the film, and conformation change are the mechanisms for the tremendous conductivity enhancement. This work will add up to the existing knowledge on conductivity enhancement of PEDOT:PSS and opens up new insights to further boost its conductivity. Up to 62% of PSS was removed after rinsing. ITO-free PSCs with standalone PEDOT:PSS anodes treated with formic acid using P3HT:PCBM as the active layer showed PCE of 4.10%, while the ITO counterpart showed 4.11%. These results demonstrate that formic acid treatment of PEDOT:PSS is highly promising for transparent flexible electrodes to replace ITO for low cost and flexible printable electronics.

■ ASSOCIATED CONTENT

Supporting Information

SEM images, XPS spectra, AC-2 photoelectron graphs and solar cell efficiency stability graph and tables showing dc conductivity to optical conductivity ratios and PEDOT to PSS ratios of PEDOT:PSS films. This material is available free of charge via the Internet at http://pubs.acs.org.

■ AUTHOR INFORMATION

Corresponding Author

*Phone: 886-2-27898000 ext 70. Fax: 886-2-27896680. E-mail: gchu@gate.sinica.edu.tw.

Notes

The authors declare no competing financial interest.

■ ACKNOWLEDGMENTS

The authors would like to thank Prof. Yia-Chung Chang for the Hall Effect measurement system, Prof. Chin-Ti Chen for the alpha step surface profiler, and Prof. Yu-Tai Tao for the AC-2. This work was financially supported by the Thematic Project of Academia Sinica (AS-100-TP-A05) and the National Science Counsel (NSC 102-2221-E-029-MY2), Taiwan.

■ REFERENCES

(1) Søndergaard, R.; Hösel, M.; Angmo, D.; Larsen-Olsen, T. T.; Krebs, F. C. *Mater. Today* **2012**, *15*, 36−49.
(2) Han, T.-H.; Lee, Y.; Choi, M.-R.; Woo, S.-H.; Bae, S.-H.; Hong, B. H.; Ahn, J.-H.; Lee, T.-W. *Nat. Photonics* **2012**, *6*, 105−110.
(3) Tao, C. S.; Jiang, J.; Tao, M. *Sol. Energy Mater. Sol. Cells* **2011**, *95*, 3176−3180.
(4) Chipman, A. *Nature* **2007**, *449*, 131−131.
(5) Azzopardi, B.; Emmott, C. J. M.; Urbina, A.; Krebs, F. C.; Mutale, J.; Nelson, J. *Energy Environ. Sci.* **2011**, *4*, 3741−3753.
(6) Cui, J.; Wang, A.; Edleman, N. L.; Ni, J.; Lee, P.; Armstrong, N. R.; Marks, T. J. *Adv. Mater.* **2001**, *13*, 1476−1480.
(7) Zhu, R.; Chung, C.-H.; Cha, K. C.; Yang, W.; Zheng, Y. B.; Zhou, H.; Song, T.-B.; Chen, C.-C.; Weiss, P. S.; Li, G.; Yang, Y. *ACS Nano* **2011**, *5*, 9877−9882.
(8) Lee, J.-Y.; Connor, S. T.; Cui, Y.; Peumans, P. *Nano Lett.* **2008**, *8*, 689−692.
(9) Tu, K.-H.; Li, S.-S.; Li, W.-C.; Wang, D.-Y.; Yang, J.-R.; Chen, C.-W. *Energy Environ. Sci.* **2011**, *4*, 3521−3526.
(10) Wu, Z.; Chen, Z.; Du, X.; Logan, J. M.; Sippel, J.; Nikolou, M.; Kamaras, K.; Reynolds, J. R.; Tanner, D. B.; Hebard, A. F.; Rinzler, A. G. *Science* **2004**, *305*, 1273−1276.
(11) Gruner, G. *J. Mater. Chem.* **2006**, *16*, 3533−3539.
(12) Gomez De Arco, L.; Zhang, Y.; Schlenker, C. W.; Ryu, K.; Thompson, M. E.; Zhou, C. *ACS Nano* **2010**, *4*, 2865−2873.
(13) Bae, S.; Kim, H.; Lee, Y.; Xu, X.; Park, J. S.; Zheng, Y.; Balakrishnan, J.; Lei, T.; Kim, H. R.; Song, Y. I.; Kim, Y. J.; Kim, K. S.; Ozyilmaz, B.; Ahn, J. H.; Hong, B. H.; Iijima, S. *Nat. Nanotechnol.* **2010**, *5*, 574−8.
(14) Gustafsson, G.; Cao, Y.; Treacy, G. M.; Klavetter, F.; Colaneri, N.; Heeger, A. J. *Nature* **1992**, *357*, 477−479.
(15) Zhang, F.; Johansson, M.; Andersson, M. R.; Hummelen, J. C.; Inganäs, O. *Adv. Mater.* **2002**, *14*, 662−665.
(16) Xia, Y.; Sun, K.; Ouyang, J. *Energy Environ. Sci.* **2012**, *5*, 5325−5332.
(17) Ouyang, J.; Chu, C. W.; Chen, F. C.; Xu, Q.; Yang, Y. *Adv. Funct. Mater.* **2005**, *15*, 203−208.
(18) Wang, P.-C.; Liu, L.-H.; Alemu Mengistie, D.; Li, K.-H.; Wen, B.-J.; Liu, T.-S.; Chu, C.-W. *Displays* **2013**, *34*, 301−314.
(19) Wei, H.-Y.; Huang, J.-H.; Hsu, C.-Y.; Chang, F.-C.; Ho, K.-C.; Chu, C.-W. *Energy Environ. Sci.* **2013**, *6*, 1192−1198.
(20) Groenendaal, L.; Jonas, F.; Freitag, D.; Pielartzik, H.; Reynolds, J. R. *Adv. Mater.* **2000**, *12*, 481−494.
(21) Kirchmeyer, S.; Reuter, K. *J. Mater. Chem.* **2005**, *15*, 2077−2088.
(22) Po, R.; Carbonera, C.; Bernardi, A.; Tinti, F.; Camaioni, N. *Sol. Energy Mater. Sol. Cells* **2012**, *100*, 97−114.
(23) Huang, J.-H.; Kekuda, D.; Chu, C.-W.; Ho, K.-C. *J. Mater. Chem.* **2009**, *19*, 3704−3712.
(24) Huang, J.; Miller, P. F.; Wilson, J. S.; de Mello, A. J.; de Mello, J. C.; Bradley, D. D. C. *Adv. Funct. Mater.* **2005**, *15*, 290−296.
(25) Nardes, A. M.; Kemerink, M.; de Kok, M. M.; Vinken, E.; Maturova, K.; Janssen, R. A. J. *Org. Electron.* **2008**, *9*, 727−734.
(26) Zhou, Y.; Cheun, H.; Choi, S.; Potscavage, J. W. J.; Fuentes-Hernandez, C.; Kippelen, B. *Appl. Phys. Lett.* **2010**, *97*, 153304−3.
(27) Reyes-Reyes, M.; Cruz-Cruz, I.; Lopez-Sandoval, R. *J. Phys. Chem. C* **2010**, *114*, 20220−20224.
(28) Badre, C.; Marquant, L.; Alsayed, A. M.; Hough, L. A. *Adv. Funct. Mater.* **2012**, *22*, 2723−2727.
(29) Ko, C.-J.; Lin, Y.-K.; Chen, F.-C.; Chu, C.-W. *Appl. Phys. Lett.* **2007**, *90*, 063509−3.
(30) Mengistie, D. A.; Wang, P.-C.; Chu, C.-W. *J. Mater. Chem. A* **2013**, *1*, 9907−9915.
(31) Alemu, D.; Wei, H.-Y.; Ho, K.-C.; Chu, C.-W. *Energy Environ. Sci.* **2012**, *5*, 9662−9671.
(32) Xia, Y.; Ouyang, J. *Org. Electron.* **2010**, *11*, 1129−1135.
(33) Xia, Y.; Ouyang, J. *ACS Appl. Mater. Interfaces* **2010**, *2*, 474−483.
(34) Xia, Y.; Zhang, H.; Ouyang, J. *J. Mater. Chem.* **2010**, *20*, 9740−9747.
(35) Xia, Y.; Ouyang, J. *J. Mater. Chem.* **2011**, *21*, 4927−4936.
(36) Kim, Y. H.; Sachse, C.; Machala, M. L.; May, C.; Müller-Meskamp, L.; Leo, K. *Adv. Funct. Mater.* **2011**, *21*, 1076−1081.
(37) Xia, Y.; Sun, K.; Ouyang, J. *Adv. Mater.* **2012**, *24*, 2436−40.
(38) Fabretto, M. V.; Evans, D. R.; Mueller, M.; Zuber, K.; Hojati-Talemi, P.; Short, R. D.; Wallace, G. G.; Murphy, P. J. *Chem. Mater.* **2012**, *24*, 3998−4003.
(39) Takano, T.; Masunaga, H.; Fujiwara, A.; Okuzaki, H.; Sasaki, T. *Macromolecules* **2012**, *45*, 3859−3865.
(40) Wei, Q.; Mukaida, M.; Naitoh, Y.; Ishida, T. *Adv. Mater.* **2013**, *25*, 2831−2836.
(41) Yoo, J. E.; Lee, K. S.; Garcia, A.; Tarver, J.; Gomez, E. D.; Baldwin, K.; Sun, Y.; Meng, H.; Nguyen, T. Q.; Loo, Y. L. *Proc. Natl. Acad. Sci. U.S.A.* **2010**, *107*, 5712−7.
(42) Kim, J. Y.; Jung, J. H.; Lee, D. E.; Joo, J. *Synth. Met.* **2002**, *126*, 311−316.
(43) Gillespie, R. J.; Cole, R. H. *Trans. Faraday Soc.* **1956**, *52*, 1325−1331.
(44) Riddick, J. A.; Bunger, W. B.; Sakano, T. K. *Organic Solvents: Physical Properties and Methods of Purification*, 4th ed.; Wiley-Interscience: New York, 1986; p 1325.

(45) Kittle, C. *Introduction to Solid State Physics*, 8th ed.; John Wiley & Sons, Inc.: Hoboken, 2005; p 208.
(46) Scardaci, V.; Coull, R.; Coleman, J. N. *Appl. Phys. Lett.* **2010**, *97*, 023114−3.
(47) Crispin, X.; Jakobsson, F. L. E.; Crispin, A.; Grim, P. C. M.; Andersson, P.; Volodin, A.; van Haesendonck, C.; Van der Auweraer, M.; Salaneck, W. R.; Berggren, M. *Chem. Mater.* **2006**, *18*, 4354−4360.
(48) Na, S.-I.; Wang, G.; Kim, S.-S.; Kim, T.-W.; Oh, S.-H.; Yu, B.-K.; Lee, T.; Kim, D.-Y. *J. Mater. Chem.* **2009**, *19*, 9045−9053.
(49) Lang, U.; Müller, E.; Naujoks, N.; Dual, J. *Adv. Funct. Mater.* **2009**, *19*, 1215−1220.
(50) Ouyang, J.; Xu, Q.; Chu, C.-W.; Yang, Y.; Li, G.; Shinar, J. *Polymer* **2004**, *45*, 8443−8450.
(51) Aleshin, A.; Kiebooms, R.; Menon, R.; Heeger, A. J. *Synth. Met.* **1997**, *90*, 61−68.
(52) Gong, C.; Yang, H. B.; Song, Q. L.; Lu, Z. S.; Li, C. M. *Sol. Energy Mater. Sol. Cells* **2012**, *100*, 115−119.
(53) de Jong, M. P.; van Ijzendoorn, L. J.; de Voigt, M. J. A. *Appl. Phys. Lett.* **2000**, *77*, 2255−2257.